JNeurosci
THE JOURNAL OF NEUROSCIENCE

Research Articles: Systems/Circuits

The hierarchy of coupled sleep oscillations reverses with aging in humans

https://doi.org/10.1523/JNEUROSCI.0586-23.2023

Cite as: J. Neurosci 2023; 10.1523/JNEUROSCI.0586-23.2023

Received: 29 March 2023
Revised: 11 July 2023
Accepted: 31 July 2023

The hierarchy of coupled sleep oscillations reverses with aging in humans

Marc Alain Züst[1]*, Christian Mikutta[2,3,4], Ximena Omlin[2], Tatjana DeStefani[2], Marina Wunderlin[1], Céline Jacqueline Zeller[1], Kristoffer Daniel Fehér[2,5], Elisabeth Hertenstein[2], Carlotta L. Schneider[2], Charlotte Elisabeth Teunissen[6], Leila Tarokh[2,7], Stefan Klöppel[1], Bernd Feige[8], Dieter Riemann[8], Christoph Nissen[2,5]

[1] University Hospital of Old Age Psychiatry and Psychotherapy, University of Bern, Bern, Switzerland
[2] University Hospital of Psychiatry and Psychotherapy, University of Bern, Bern, Switzerland
[3] Private Clinic Meiringen, Meiringen, Switzerland
[4] Department of Physiology, Anatomy and Genetics, University of Oxford, Oxford, United Kingdom
[5] Division of Psychiatric Specialties, Geneva University Hospitals (HUG), Geneva, Switzerland
[6] Neurochemistry Laboratory, Department of Clinical Chemistry, Amsterdam Neuroscience, Neurodegeneration, Vrije Universiteit Amsterdam, Amsterdam UMC, Amsterdam, Netherlands
[7] University Hospital of Child and Adolescent Psychiatry and Psychotherapy University of Bern, Switzerland
[8] Department of Psychiatry & Psychotherapy, University of Freiburg Medical Center, Freiburg, Germany

Number of pages: 34

Number of figures: 4 Number of tables: 1

Number of words: 245 (Abstract) 954 (Introduction) 1727 (Discussion)

Conflicts of interest

CN has served on advisory boards of Idorsia, Lundbeck and Janssen. The other authors have no conflict of interest to declare.

Acknowledgements

This work was supported by the Dementia Research: Synapsis Foundation Switzerland, in collaboration with the Peter Bockhoff Foundation, the Heidi Seiler Foundation, and the Kurt Fries Foundation [grants No. 2018-PI02 to SK, CN, MZ and MW, and 2021-CDA03 to MZ]. The funding agencies had no role in conceptualization, design or analysis plan of this research.

* Please address correspondence to:
Marc Alain Züst, PhD
University Hospital of Old Age Psychiatry and Psychotherapy
Bolligenstrasse 111, 3000 Bern 60, Switzerland
Tel.: +41 (0)31 930 89 03
e-mail: marc.zuest@upd.unibe.ch

Abstract

A well-orchestrated coupling hierarchy of slow waves and spindles during slow wave sleep supports memory consolidation. In old age, duration of slow wave sleep and number of coupling events decreases. The coupling hierarchy deteriorates, predicting memory loss and brain atrophy. Here, we investigate the dynamics of this physiological change in slow wave-spindle coupling in a frontocentral electroencephalography position in a large sample (N=340, 237 female, 103 male) spanning most of the human lifespan (ages 15-83). We find that, instead of changing abruptly, spindles gradually shift from being driven by-, to driving slow waves with age, reversing the coupling hierarchy typically seen in younger brains. Reversal was stronger the lower the slow wave frequency, and starts around midlife (~age 40-48), with an established reversed hierarchy at age 56-83. Notably, coupling strength remains unaffected by age. In older adults, deteriorating slow wave-spindle coupling, measured using phase slope index (PSI) and number of coupling events, is associated with blood plasma glial fibrillary acidic protein (GFAP) levels, a marker for astrocyte activation. Data-driven models suggest decreased sleep time and higher age lead to fewer coupling events, paralleled by increased astrocyte activation. Counterintuitively, astrocyte activation is associated with a back-shift of the coupling hierarchy (PSI) towards a “younger” status along with increased coupling occurrence and strength, potentially suggesting compensatory processes. As the changes in coupling hierarchy occur gradually starting at midlife, we suggest there exists a sizable window of opportunity for early interventions to counteract undesirable trajectories associated with neurodegeneration.

Keywords: Slow wave sleep, sleep spindles, phase-amplitude coupling, aging, astrocyte activation, biomarkers, neurodegeneration, human life-span

Significance Statement

Evidence accumulates that sleep disturbances and cognitive decline are bi-directionally and causally linked forming a vicious cycle. Improving sleep quality could break this cycle. One marker for sleep quality is a clear hierarchical structure of sleep oscillations. Previous studies showed that sleep oscillations decouple in old age. Here, we show that, rather, the hierarchical structure gradually shifts across the human lifespan and reverses in old age, while coupling strength remains unchanged. This shift is associated with markers for astrocyte activation in old age. The shifting hierarchy resembles brain maturation, plateau, and wear processes. This study furthers our comprehension of this important neurophysiological process and its dynamic evolution across the human lifespan.

1. Introduction

Sleep is of central importance for the brain, promoting vital functions like memory consolidation, synaptic renormalization, and clearance of metabolic waste-products like amyloid beta (Aβ), a hallmark for Alzheimer's disease (Mander et al., 2016; Rasch & Born, 2013; Tononi & Cirelli, 2020; Xie et al., 2013). Coupled oscillations, especially during slow wave sleep (SWS), have been identified as a cornerstone of the function of sleep for the brain. Neocortical slow waves (SW, <1.25 Hz), thalamo-cortical spindles (12-16 Hz) and hippocampal sharp-wave ripples (80-100 Hz) are hierarchically orchestrated to allow for optimized, synchronized information processing that enables memory consolidation (Rasch & Born, 2013; Staresina et al., 2015). For optimal functionality, the layers of this hierarchy are organized in a relationship of phase-amplitude coupling, where the faster spindles are nested into the depolarizing up-phase of the slower SW. This allows for synchronized, widespread communication during periods of high responsiveness and therefore efficient top-down control of processes like memory consolidation (Bastian et al., 2022; Helfrich et al., 2018; Mikutta et al., 2019; Rasch & Born, 2013; Tort et al., 2010).

With age, sleep quality and quantity declines, leading to a loss of SWS (Mander et al., 2017). This loss inevitably entails less opportunity for sleep's important functions. While part of normal aging (Carrier et al., 2011; Hertenstein et al., 2018), this loss is more severe in neurodegenerative disorders, like Alzheimer's disease (Rauchs et al., 2008; Westerberg et al., 2012; Zhang et al., 2022). As neurodegeneration progresses, sleep quality declines, which in turn robs the brain of crucial recuperative functions, worsening neurodegeneration (Mander et al., 2016). With lacking SWS, Aβ is not cleared from the brain as effectively, and the residual Aβ in turn disrupts sleep (Eide et al., 2021; Fultz et al., 2019; Ju et al., 2017; Kang et al., 2009; Mander et al., 2015; Roh et al., 2012; Varga et al., 2016; Winer et al., 2019, 2020), leading to a vicious cycle (Mander et al., 2016; Wunderlin et al., 2020; Zeller et al., 2023).

The orchestrated coupling of spindles and SW follows along with these age-related sleep changes. Recent studies posit that spindles become uncoupled from SW in the aging brain, and this change is associated with degrading memory and medial frontal brain atrophy (Helfrich et al., 2018; Muehlroth et al., 2019). In younger individuals, SW drive spindles, signifying that SW inhabit a higher position in

the hierarchy of coupled oscillations. In older individuals, however, this clear cross-frequency directionality deteriorates (Helfrich et al., 2018).

Importantly, it is known that older individuals with higher structural brain integrity in areas like the medial prefrontal cortex and hippocampus exhibit a SW-spindle coupling physiology reminiscent of a younger brain (Muehlroth et al., 2019). Moreover, enhancing SW-spindle coupling using transcranial electric stimulation has been shown to improve post-sleep declarative memory retrieval in older adults with mild cognitive impairment (Ladenbauer et al., 2017), suggesting the unfavorable age-associated deterioration of SW-spindle coupling can potentially be compensated to prevent cognitive decline.

While currently available research paints quite a stark contrast between younger and older adults, it is not clear how and when these changes emerge. Are changes in SW-spindle coupling gradually appearing across the adult human lifespan, or suddenly at a specific age? At what age does the process become apparent? Here, we address these open questions by examining SW-spindle coupling in an extensive sample (N=340) spanning a large portion of the human lifespan (age 15-83). Instead of focusing on group differences between younger and older individuals including all associated cross-generational inhomogeneity, we investigate SW-spindle coupling as a continuum across the human lifespan.

When aiming to prevent cognitive decline, early detection of unfavorable trajectories is key. Recently, blood-based biomarker assessments have become an affordable, minimally invasive approach for the early prediction of cognitive decline (Beyer et al., 2022; Thijssen et al., 2021; Verberk et al., 2020). The most promising prognostic blood-based biomarkers currently discussed are Aβ42/40 ratio and glial fibrillary acidic protein (GFAP) levels. A lower blood Aβ42/40 ratio is thought to be a marker for impaired clearance of Aβ from the brain. Increased levels of GFAP is a marker for astrocyte activation, with a potential role in neuroinflammation due to neuronal damage or degeneration (Thijssen et al., 2021; Verberk et al., 2020). Experimentally induced sleep deprivation is linked with astrocyte activation and neuroinflammation as indicated by increased cytokine and GFAP levels in rodents (Manchanda et al., 2018; Xiao et al., 2022). High GFAP levels are associated with a steeper rate of decline in memory, executive functioning and attention, and had a high prognostic value for incident dementia in humans (Verberk et al., 2021). Using a combination of amyloid misfolding status

and GFAP levels, the incidence of Alzheimer's diagnosis could be accurately predicted 17 years in advance with receiver-operating characteristic area under the curve of .83 (Beyer et al., 2022), paving the way for minimally invasive early detection of cognitive decline.

In addition to investigating the dynamics of the shift in SW-spindle coupling across the human lifespan, we examine if changes in the hierarchical coupling structure of brain oscillations during slow wave sleep are reflective of neuronal degradation as measured by blood-based biomarkers. For this purpose, we analyze associations of SW-spindle coupling with readily accessible blood-based biomarkers for dementia and astrocyte activation (Aβ42/40 ratios and GFAP levels) in a subgroup of older individuals.

A continuous investigation of brain physiology from adolescence to senescence allows for a deeper understanding of the dynamic processes the brain undergoes throughout our lifetime. It can put individual neurophysiological characteristics into context, allows us to better identify pathological trajectories, and separate pathological from healthy trajectories. This knowledge can accelerate the development of tailored treatment- and prevention methods for cognitive decline, especially as more early warning signs are identified every year.

2. Methods

2.1. Sample

The total sample consisted of 340 whole-night baseline sleep recordings of healthy participants (237 female, 103 male, age: 15-83, *M*±*SD*: 43.4±17.8, see Table 1) participating in various studies at the Department of Psychiatry and Psychotherapy, University of Freiburg Medical Center (UFMC) between 2008 and 2018 and University Hospital for Old Age Psychiatry and Psychotherapy Bern (UPD) between 2019 and 2021. Of the total sample, 310 participants were measured at UFMC (213 female, age: 15-83, *M*±*SD*: 40.9±16.5) and 30 participants were measured at UPD (24 female, age: 61-80, *M*±*SD*: 69.5±4.3). All participants underwent extensive screening procedures to confirm suitability as healthy study participants, which was the first inclusion criterion. The second inclusion criterion was availability of polysomnographic (PSG) recordings of an entire night under baseline measurement

conditions after an adaptation night – i.e., natural sleep with no intervention. Exclusion criteria were current or recent (over the last 6 months) psychiatric or physical illness, especially if impacting sleep (e.g., insomnia, hypersomnia, sleep apnea syndrome, or restless legs syndrome), irregular sleep patterns, substance abuse, use of prescription medication acting on the central nervous system, and pregnancy. Studies were conducted in accordance with the Declaration of Helsinki as approved by local ethics committees. All individuals (and their parents if underage) gave written informed consent.

2.2. Procedures

All participants completed one night of PSG. At UFMC, sleep was recorded on a 24-channel EEG PSG device with a sampling rate of 200 or 256 Hz. Recorded EEG channels included C3, C4, Fz, Fpz, and Oz. During recording, channels C3 and C4 were referenced against contralateral mastoids, the other channels were referenced against pooled mastoids or Cz. More information about UFMC data, infrastructure and standard procedures can be found elsewhere (Hertenstein et al., 2018). At UPD, sleep was recorded using a high-density EEG system (128-channel MicroCel Geodesic Sensor Net, 16-channel Physio16 input box, 400 Series Geodesic EEG System™) by Magstim EGI (Eugene, OR, USA), with a sampling rate of 500 Hz, referenced against Cz. Polysomnographic scoring of sleep stages was performed according to the criteria of the American Academy of Sleep Medicine (Iber et al., 2007) by experienced somnologists for all 340 datasets.

For 28 of the 30 participants in the UPD sample (22 female, age: 61-80, $M \pm SD$: 69.5±3.9), blood samples were taken in the morning (~1 hour after waking) and immediately centrifuged and stored at -80°C. The resulting plasma samples were analyzed in the Neurochemistry Lab, Amsterdam University Medical Center, Amsterdam, NL. Plasma Aβ 1-42 and 1-40, as well as GFAP levels were quantified using Simoa immunoassays (IA-N4PE)(Thijssen et al., 2021), and Aβ42/40 ratios were calculated. All measurements were above the limits of detection and the functional lower limits of quantification as per the manufacturer's specifications. High GFAP levels and low Aβ42/40 ratios constitute risk factors for neurodegenerative disease and are strongly associated with amyloid-positivity as assessed with positron-emission tomography (Graff-Radford et al., 2007; Verberk et al., 2020, 2021).

2.3. Sleep parameters

We determined the following sleep parameters individually, then averaged for the whole sample (N=340) as well as for age quartiles: Sleep period time (SPT), defined as the time from sleep onset to the final awakening (Hertenstein et al., 2018); total sleep time (TST, i.e. SPT minus intermittent wakefulness), sleep (onset) latency (SL, i.e. the time until first occurrence of non-rapid eye movement sleep stage 1), sleep efficiency (SE) as percentage of sleep during bedtime, spindle density (SD, measured as spindle events per minute of N2/N3 sleep), slow wave amplitude (SW amp, in μV, negative-to-positive peak of detected SW events), as well as standard AASM sleep architectural stages, i.e., wakefulness, non-rapid eye movement sleep stages 1 through 3 (N1-N3), and rapid eye movement (REM) sleep. SPT, TST and SL are measured in hours, sleep architectural stages in percent of SPT. For all sleep parameters, we tested association with age using Pearson's determination coefficients. A more in-depth evaluation of sleep parameters of UFMC data is reported elsewhere (Hertenstein et al., 2018).

2.4. EEG processing

EEG processing, as well as calculation and statistical analysis of SW-spindle coupling was achieved in MATLAB R2019a (Natick, Massachusetts: The MathWorks Inc.) using EEGLAB (Delorme & Makeig, 2004), the CircStat toolbox (Berens, 2009), the fieldtrip toolbox (Oostenveld et al., 2010) and the phase-amplitude coupling analysis framework by Jiang et al. (2015). For the UFMC dataset, 30-second segments of data containing artifacts were manually labelled and excluded from analysis. For the UPD dataset, EEG data was preprocessed using the PREP pipeline for EEGLAB (Bigdely-Shamlo et al., 2015) and the automatic artifact rejection pipeline as implemented in the fieldtrip toolbox (Oostenveld et al., 2010). All analyses were conducted on artifact-free N2 or N3 sleep data on channel Fz, referenced against pooled mastoids, resampled to 200 Hz if necessary.

2.5. Slow wave-, spindle- and coupling event classification

SW- and spindle events were detected using previously established methods (Helfrich et al., 2018; Mölle et al., 2009; Staresina et al., 2015). For slow oscillations, we filtered data between 0.16 and 1.25 Hz and marked zero crossings. SW events were then defined as negative peaks between two consecutive positive-to-negative zero crossings based on duration (0.8-2 seconds) and amplitude

(individual 75th percentile) criteria (Helfrich et al., 2018; Mölle et al., 2009). For sleep spindles, we filtered data between 12 and 16 Hz and extracted the amplitude of the Hilbert transform. Spindle events were defined as peaks of the smoothed (200 ms moving average) Hilbert-amplitude curve in regions that exceeded the individual 75th amplitude percentile for 0.5 to 3 seconds (Staresina et al., 2015). Spindle events that were within 2.5 seconds of a SW-event were marked as SW-coupled spindles and constitute coupling events. We then extracted the coupling phases, i.e., the instantaneous SW-phase angles of SW-coupled spindles using the angle of the Hilbert transform in SW-filtered (0.16-2 Hz) data. To counteract reduced SW power with age, we z-standardized data within participants prior to analyses of SW-spindle coupling.

2.6. Quantifying slow wave-spindle coupling

The number of coupling events yields a first measure of SW-spindle coupling and can vary with quantity (i.e., the time spent asleep) and/or quality (i.e. the exact electrophysiological synchronization of SW and spindles) of SWS. In addition to the number of coupling events, we calculated three principal SWS-quantity-independent measures of SW-spindle coupling:

1) The resultant vector angle (rvec angle), or mean circular direction (CircStat::circ_mean) of coupling phases yields a measure of the preferred coupling phase of spindles within SW. An rvec angle of 0° is equivalent to the positive peak, ±180° to the negative peak, negative values up to -90° are before a positive peak, and positive values up to 90° are after a positive peak. As rvec angle is a circular measure, its utility is limited to circular statistics, and it cannot be included in linear models.

2) The modulation index (MI) (Jiang et al., 2015; Tort et al., 2010) as a measure of cross-frequency coupling was calculated between the phase of a lower frequency (SW, 0.39-1.95 Hz in 0.39 Hz steps) and the amplitude of a higher frequency (spindles, 12-16 Hz in 1 Hz steps). The MI is a measure of circular spread and indicates how far an empirical distribution deviates from uniformity using the Kullback-Leibler divergence. The higher the MI, the more closely all coupling phases are grouped around the preferred phase, i.e., the stronger the coupling.

3) The phase slope index (PSI) (Jiang et al., 2015) as a measure of cross-frequency directionality was calculated between the phase of a lower frequency (SW, 0.5-2 Hz in 0.5 Hz steps) and the amplitude of a higher frequency (spindles, 12-16 Hz in 1 Hz steps). The PSI robustly measures the consistency

of phase lag or lead between the two frequencies, and a value significantly different from 0 is suggestive of causal influence of the leading over the lagging frequency. A positive PSI indicates SW drive spindles, a negative PSI indicates spindles drive SW. The PSI can be used instead of rvec angle in linear models.

MI and PSI were calculated on 5-second data segments centered on the negative peak of detected slow waves. We defined a sliding window of 2 seconds length with 1 second steps, using 5 cycles to estimate frequency power. We then averaged the resulting MI and PSI values for all possible frequency sub-band pairs to yield a single estimate for MI and PSI between the SW and spindle bands per subject.

As the number of coupling events diminishes with age (R^2=0.48, p<.001), lower numbers of coupling events might bias the estimation of SW-spindle coupling and its association with age. To counteract this, we implemented a per-subject bootstrapping procedure where we repeated calculation of rvec angles and MI with q randomly selected coupling events, where q equals the smallest number of coupling events across all participants (q = 120 in a subject aged 77). This random draw was repeated for 1000 iterations per subject (or, if not possible, for the maximum number of unique draws), and an average coupling measure was then calculated from the mean of the bootstrapping distribution. We used a leave-one-out jackknifing procedure to test stability of the estimation of the PSI. If estimation of the PSI exhibited low stability (|z(jackknifing error)| > 2), the subject was excluded from PSI analyses, which was the case in 9/340 participants. These unstable estimates contained three outliers (|z(PSI)| > 3), and no outliers remained after exclusion of unstable estimates.

2.7. Testing for association of slow wave-spindle coupling and age

We tested for associations of measures of SW-spindle coupling (number of coupling events, rvec angle, MI and PSI) with age. For linear coupling measures (number of coupling events, MI and PSI) we calculated the Pearson correlation coefficient with age. For preferred coupling phase (rvec angle), we used CircStat::circ_corrcl for a circular-linear correlation between rvec angle and age. Importantly, an rvec angle can technically be calculated even in almost uniformly distributed data, but would not produce a sensible estimate of preferred phase in that case. Therefore, we repeated the circular-linear correlation between rvec angle and age, as well as the linear correlation between PSI and age,

in a subset of individuals exhibiting high coupling strength as measured by MI to minimize bias due to invalid estimations of preferred phase. As MI was right-skewed, we defined high MI as z(ln(MI))>0, which was the case in 177 participants. This logarithmic transformation normalizes the distribution of MI and allows z-transformed values above 0 to represent the upper half of MI data. For effect sizes, we calculated explained variance through determination coefficients (R^2).

For significant associations of SW-spindle coupling with age (rvec angle and PSI), we further subdivided the sample into age quartiles and tested the quartiles separately against zero. Preferred coupling phase (rvec angle) was tested against zero using a one sample test for mean angle (CircStat::circ_mtest). Zero was chosen as test value because it marks the highest point on a positive SW peak; thus allowing to test if spindles prefer to nest significantly before or after a SW peak. PSI was tested against zero using one-sample t-tests. Zero was chosen as test value because it marks the reversal-point of cross-frequency directionality, i.e., a reversal of which frequency drives the other. We additionally calculated the x-zero-crossing of the best-fit models of the association between SW-spindle coupling measures and age to estimate the age at which a reversal happens. For MI, we tested age quartiles against each other in an ANOVA to test for potential non-linear shifts in coupling strength between age quartiles.

To account for potential sources of bias, we calculated a linear regression of age on PSI (Matlab::lmfit) and let a data-driven stepwise procedure (Matlab::step) optimize this model by testing change in model fit by the inclusion and exclusion of terms. Each step, the term yielding the highest gain in R^2 is added, provided R^2 would increase by at least 0.1. Gender, age, linear coupling measures, SW up- and down-phase duration, number of coupling events, sleep parameters (TST, SL, SPT in hours; stages N1-3 & REM, as well as intermittent wakefulness in % SPT, SD, SE, and SW amplitude) and interactions of existing terms may be added as factors if not already present. If no term can be added this way, the term resulting in the least loss of R^2 is removed provided R^2 would decrease by no more than 0.05. If neither threshold is met through further changes in the model, the procedure ends. Final models were *F*-tested against intercept-only models. To prevent overfitting, model R^2 was adjusted for the number of included terms. To explicitly test for an influence of up- and down-phase duration on coupling, an additional model was calculated to include up- and down-phase duration a-priori. To explicitly test for gender differences, an additional model was calculated to

include gender a-priori. For these models, the ΔR^2 threshold for excluding terms was set more liberally at 0.02 to allow control for gender and SW duration effects even if they are small. All model optimizations finished within four steps.

2.8. Blood biomarker analysis

For 28 participants in the UPD sample, blood-based biomarkers were analyzed for associations with SW-spindle coupling while controlling for potential confounders such as gender, age and sleep parameters. Initially, a-priori baseline models were defined explaining blood biomarkers (Aβ42/40 ratios and GFAP levels) by linear coupling measures (number of coupling events, MI, and PSI) and age, and explaining linear coupling measures by blood biomarkers and age. Stepwise optimization allowed for the inclusion and exclusion of gender, age, blood biomarkers, linear coupling measures, sleep parameters and interactions as described above (section 2.7). All model optimizations finished within three steps.

2.9. Data availability

Data will be deposited on an open repository (e.g., https://boris-portal.unibe.ch/) upon article acceptance.

3. Results

3.1. Trends for sleep parameters across the human lifespan replicate earlier findings

Consistent with earlier studies (Carrier et al., 2011; Hertenstein et al., 2018), the structure of sleep changes with age (table 1). We found significant decreases in sleep period time (SPT, R^2=.14), total sleep time (TST, R^2=.43), proportional non-rapid eye movement sleep (N) stages N3 (R^2=.38) and rapid eye movement sleep (REM, R^2=.18) sleep, as well as spindle density (R^2=0.41), SW amplitude (R^2=0.25), and the number of coupling events (R^2=0.48) with age (p<.001). Conversely, N1 sleep (R^2=.31) and periods of intermittent wakefulness (R^2=.37) were increased (p<.001) with age. Sleep onset latency (SL) and stage N2 did not change with age (R^2<.01, n.s.).

TABLE 1 ABOUT HERE

3.2. Spindle density, age, and total sleep time determine number of slow wave-spindle coupling events

With age the number of coupling events is strongly reduced (R^2=0.48, p<.001, see table 1). A stepwise optimized linear regression model (F(338)=1910, R^2_{adj}=.85, p<.001) indicated that number of coupling events is best explained by spindle density (t=43.69, p<.001), an association so strong no other factors were being considered. If spindle density is removed from the pool of available regressors, an optimized model (F(337)=282, R^2_{adj}=.62, p<.001) indicated that number of coupling events is best explained by age (t=-8.24, p<.001) and TST (t=11.51, p<.001). It is therefore difficult to isolate the effect of age on SW-spindle coupling measures (rvec angle, MI, and PSI) from reduced numbers of coupling events due to reduced spindle density. To counteract this, we implemented bootstrapping and jackknifing procedures (see Methods – Quantifying slow wave-spindle coupling) to test robustness of age effects on SW-spindle coupling measures against variance in number of coupling events. This allows the evaluation of age-related effects on SW-spindle coupling while number of coupling events is held constant. Notably, all results regarding age effects in rvec angle, MI, and PSI are unchanged whether these procedures are implemented or not.

3.3. Spindles shift from lagging to leading slow waves without loss of coupling strength with age

Spindles prefer to nest into the positive half-wave of the SW for almost all participants across all ages, as 338/340 (>99%) of individual rvec angles lay within SW-phase angles of -90° and +90°. However, with age, the average preferred coupling angle shifts from after to before the peak of the SW. This is indicated by a significant circular-linear correlation of rvec angle and age (r=.57, p<.001), with age explaining 33% of variance in rvec angle. For the youngest age-quartile (Q1), the average preferred coupling phase occurs significantly after peak (M=24.8°, CI_{95}=[15.9°, 33.7°], p<.001), while for the oldest age-quartile (Q4), the average preferred coupling phase occurs significantly before the peak (M=-22.0°, CI_{95}=[-35.7°, -8.3°], p<.01). Age quartiles Q2 and Q3 did not exhibit significant deviations of rvec angle from 0°. The best-fit model suggests a reversal of preferred spindle coupling from after- to before the SW peak at age 43.9 (fig. 1C).

The age-dependent forward-shifting of preferred spindle-coupling phase within SW becomes even more pronounced if participants exhibiting weak coupling are excluded. We repeated the circular-linear correlation of rvec angle and age only in participants exhibiting a high MI between SW and spindle frequencies. High MI was defined as z(ln(MI))>0 (data above the red dotted line in fig. 1B), yielding a subgroup of N_{highMI}=177. The resulting correlation was highly significant (r=.65, p<.001) with age explaining 42% of variance in rvec angle, which is significantly higher than using the entire sample (Pearson & Filon's z: -12.58, p<.001). In this high MI subgroup, age quartiles Q1 (M=20.6°, CI_{95}=[7.9°, 33.3°], p<.001), Q3 (M=-6.9°, CI_{95}=[-12.2°, -1.6°], p<.05) and Q4 (M=-24.3°, CI_{95}=[-43.3°, -5.2°], p<.001) show significant deviations of preferred coupling from the peak of the SW (0°), with a best-fit model suggested reversal at age 40.4 (fig. 1D).

The observed forward-shift of preferred coupling phase with age manifested in a reversal of cross-frequency directionality. While in younger adults, SW drive spindles, in older adults, spindles drive SW. This is illustrated by a significant correlation of PSI and age (r=-.19, p<.001). However, this measure allowing stronger claims exhibits higher variance compared to preferred coupling phase using rvec angles, with age explaining only 3% of the variance in PSI. Notably, there was a shift in SW peak frequency across age, manifesting in a slightly increased duration of up-phase (R^2=0.01, p=.012), and a markedly increased duration of down-phase (R^2=0.26, p<.001) of SW events in line with previous reports (Carrier et al., 2011). Up- (r=.29, p<.001), but not down-phase (r=-.05, p=.408) duration was correlated with PSI. PSI is inherently capable of addressing shifting frequency peaks (Jiang et al., 2015), especially since we chose a wider window for lower frequency between 0.5 and 2.0 Hz to allow for individual drifts. Still, this age-related shift in SW frequency may confound calculation of age-related trends in coupling. To account for this, we ran a stepwise optimized regression analysis initially including both up- and down-phase duration of SW events as regressors. During optimization, down-phase duration was removed as regressor, yielding a final model that revealed an improved effect of age on PSI (F(328)=21.7, R^2_{adj}=.11, p<.001, age $R^2_{partial}$=.05), indicating varying SW frequency with age partially masked the effect of age on PSI.

Some studies suggest gender to be an interacting factor in age-associated changes in SWS (Ohayon et al., 2004; Redline et al., 2004) and therefore, gender could influence age-associated changes in SW-spindle coupling. Our stepwise regression optimization procedures were allowed to control for

gender, but never included gender as a factor because it did not explain enough variance to pass the entry threshold. Still, we wanted to explicitly test for effects of gender using gender as a-priori regressor in a model explaining PSI by age and optimized this model stepwise using a more liberal threshold to keep terms (see Methods, section 2.7). This model still showed a significant effect of age on PSI ($F(328)=6.3$, $R^2_{adj}=.031$, $p=.002$, age $R^2_{partial}=.032$) with gender having almost no influence ($p=.62$). Stepwise optimization reverted to the model above, removing gender but including SW up-phase duration.

Similarly, the COVID-19 pandemic may have influenced sleep quality of participants enrolled in years 2020/21. We repeated the procedure described above for gender, substituting gender for a regressor coding whether study participation occurred during the pandemic (true for 24 participants). This analysis yielded similar results, showing no effect of pandemic ($p=.83$) on the significant age-related change in PSI ($F(328)=6.2$, $R^2_{adj}=.031$, $p=.002$, age $R^2_{partial}=.029$). Again, stepwise optimization reverted to the model only including age and SW up-phase duration.

Importantly, age quartiles Q2 ($M=0.0011$, $CI_{95}=[0.0004, 0.0017]$, $t(87)=3.29$, $p=.001$) and Q4 ($M=-0.0011$, $CI_{95}=[-0.0017, -0.0005]$, $t(88)=-3.44$, $p<.001$) exhibit significant deviations of PSI from 0, including a sign-flip, indicating a reversal of which frequency drives the other at best-fit model suggested age 43.2 (fig. 1E).

Interestingly, the youngest age quartile did not exhibit a significant PSI, indicating no clear cross-frequency directionality in the age group 15-26. To investigate a potential rising and falling relationship between age and PSI, a stepwise linear model was allowed to fit higher-order polynomial age terms. To prevent overfitting in data-sparse regions, four data at age >73 were removed from this model. Including a cubic polynomial peaking at age 29.2 resulted in the best model fit, increasing explained variance (ΔAIC vs. linear: -11.95, $F(323)=9.32$, $R^2_{adj}=.07$, $p<.001$). This model suggests a reversal of which frequency drives the other at age 47.7 (fig. 1E, blue curve).

As with rvec angle, the age-dependent shift of PSI, including a sign-flip, becomes more pronounced if only participants exhibiting strong coupling (high MI) are included (fig. 1F). As with rvec angle, high MI was defined as $z(\ln(MI))>0$, yielding a subgroup of $N_{highMI}=172$. In this subgroup, the association of age and PSI became stronger, about doubling explained variance. A linear correlation yielded $R^2=.07$

(*p*<.001), which is significantly stronger than including the entire sample (Pearson & Filon's z: 33.14, *p*<.001). This association was again improved by including SW up-phase duration as predictor in a linear regression ($F(169)=19.9$, $R^2_{adj}=.18$, $p<.001$, age $R^2_{partial}=.09$), and showed an even stronger cubic relationship (ΔAIC vs. linear: -13.93, $F(168)=10.50$, $R^2_{adj}=.15$, $p<.001$). A suggested reversal of which frequency drives the other was between ages 44.5 (linear) and 48.1 (cubic). This was again paralleled by age quartiles Q2 ($M=0.0019$, $CI_{95}=[0.0009, 0.0030]$, $t(44)=3.74$, $p<.001$) and Q4 ($M=-0.0022$, $CI_{95}=[-0.0033, -0.0012]$, $t(42)=-4.35$, $p<.001$) exhibiting significant and opposite deviations of PSI from 0.

While SW-spindle coupling clearly shifts across the human lifespan, reversing the coupling hierarchy around age 40-48, coupling strength remains unaffected. This is illustrated by the absence of an association of MI and age ($R^2<10^{-4}$, $p=.84$, fig. 1B). An ANOVA on MI age quartiles did not yield a significant effect ($F(3,336)=1.32$, $p=.267$). Pairwise comparisons showed a trend of Q2>Q4 ($t(84)=1.82$, $p=.070$), which is reminiscent of previous findings (Helfrich et al., 2018), but this result is not robust and should be treated as a negative finding. In addition, the age groups where the effect seems to occur are not directly comparable (Helfrich et al.'s younger group's age was 20.4±2.0 years, *M*±*SD*, while our Q2's age was 38.2±6.3 years). Alternatively, the right-skewed nature of MI, combined with higher variance in the middle age quartiles compared to Q1/4 (Bartlett's $\chi^2=34.93$, $p<.001$) may cause the appearance of changing means.

FIGURE 1 ABOUT HERE

3.4. The lower the slow wave frequency, the stronger slow wave-spindle coupling and reversal of information flow

To more closely investigate the exact nature of SW-spindle coupling and the observed reversal of information flow (from SW leading spindles to vice versa) with age, we re-ran the regression analyses of age on PSI for SW subbands (0.5, 1.0, 1.5, and 2.0 Hz) separately. A 4×4 repeated-measures ANOVA with the factors "SW subband" and "age quartile" (Q1-Q4) revealed a significant main effect for SW subband ($F(3,981)=3.32$, $p=.033$, Greenhouse-Geisser corrected) and a significant interaction with age quartile ($F(9,981)=7.37$, $p<.001$). The significant interaction is due to lower SW subbands

showing a stronger age-dependent reversal effect than higher subbands. Additional FDR-corrected t-tests of single subbands against 0 indicated that significant sign-flips from positive to negative PSI (i.e., reversal of information flow) occurred for subbands 0.5 and 1.0 Hz only (cf. asterisks for age quartiles in fig. 2).

Next, we investigated age-trends for the four PSI SW subbands. For each SW subband, two models were calculated, paralleling the final models from the analysis of age on PSI in section 3.3 and figure 1E: 1) a linear model including SW up-phase duration as covariate; 2) a model including up to cubic terms of age. The strongest age-related PSI shift occurred for the lowest SW subband, 0.5 Hz (linear: $F(328)=28.4$, $R^2_{adj}=.14$, $p<.001$, age $R^2_{partial}=.11$; cubic: $F(323)=17.2$, $R^2_{adj}=.13$, $p<.001$; fig. 2, left-most panel). With increasing SW subband frequency, this relationship got progressively less pronounced (1.0 Hz linear: $F(328)=24.0$, $R^2_{adj}=.12$, $p<.001$, age $R^2_{partial}=.03$; 1.0 Hz cubic: $F(323)=9.0$, $R^2_{adj}=.07$, $p<.001$; 1.5 Hz linear: $F(328)=9.1$, $R^2_{adj}=.05$, $p<.001$, age $R^2_{partial}=.01$; 1.5 Hz cubic: $F(323)=4.0$, $R^2_{adj}=.03$, $p=.008$; fig. 2, middle panels). The highest SW subband, at 2.0 Hz, was no longer significantly associated with age (linear: $F(328)=2.0$, $R^2_{adj}=.01$, $p=.132$, age $R^2_{partial}=.004$; cubic: $F(323)=1.2$, $R^2_{adj}=.001$, $p=.31$; fig 2., right-most panel). PSI exhibits markedly reduced variance in the highest SW subband (2.0 Hz), hovering around 0 (fig. 2, right most panel). This illustrates the transition away from slow wave frequencies into the upper delta range. Counterintuitively, the first two age-quartiles in the 2.0 Hz subband even exhibit significantly negative PSI, but due to the very low absolute values and variance, we treat this as a false positive finding.

FIGURE 2 ABOUT HERE

3.5. Plasma GFAP, but not plasma amyloid β42/40, is associated with slow wave-spindle coupling in older individuals

Plasma GFAP levels after waking were strongly associated with SW-spindle coupling in 28 older individuals with biomarker measurements in an optimized linear regression model ($F(25)=6.45$, $R^2_{adj}=.29$, $p=.006$). Number of coupling events ($t=-2.17$, $p=.039$) and PSI ($t=2.77$, $p=.010$) were significant predictors of GFAP levels (fig. 3). The negative association between number of coupling events and GFAP levels indicate that individuals with lower overall SWS quality and/or quantity show

increased signs of astrocyte activation. Somewhat counterintuitively, the positive association between PSI and GFAP indicates that older individuals exhibiting a more positive cross-frequency directionality typical for younger individuals (i.e., SW driving spindles rather than spindles driving SW) showed increased signs of astrocyte activation. Age and MI were dropped from the a-priori baseline model and no other terms (e.g., sleep parameters) were added during stepwise model optimization. Notably, as neither proportion of N2/N3 sleep, nor TST were considered predictors of plasma GFAP levels, the association of the number of coupling events with GFAP seems to be independent of the absolute available time (quantity) in SWS for coupling to occur, and more dependent on the quality of SWS determining whether coupling occurs or not.

The number of coupling events was best explained using an optimized model ($F(22)=5.42$, $R^2_{adj}=.45$, $p=.002$) including all a-priori terms (MI, PSI, age, and GFAP), as well as TST as strong predictor. While MI ($t=2.20$, $p=.039$) and TST ($t=3.09$, $p=.005$) significantly predicted the number of coupling events, PSI ($t=1.63$, $p=.118$), age ($t=-1.74$, $p=.096$), and GFAP levels ($t=-1.69$, $p=.106$) explained enough variance to remain in the model. Unsurprisingly, the number of coupling events increases with total sleep time (TST), illustrating its dependency upon sleep quantity. The positive association of MI and coupling events, on the other hand, explains how qualitative aspects of SWS as indicated by coupling strength are associated with an increased occurrence of coupling events.

MI was best explained using an optimized model ($F(23)=4.00$, $R^2_{adj}=.31$, $p=.013$) including the number of coupling events ($t=2.27$, $p=.033$), PSI ($t=-2.68$, $p=.013$), GFAP ($t=0.48$, $p=.638$) and the interaction of PSI*GFAP ($t=2.22$, $p=.036$). Age was removed from the model during stepwise model optimization, paralleling the result of the whole-sample analysis (N=340, fig. 1B).

PSI was best explained using an optimized model ($F(24)=3.62$, $R^2_{adj}=.23$, $p=.028$) including the number of coupling events ($t=1.36$, $p=.19$), MI ($t=-1.62$, $p=.118$), and GFAP ($t=2.54$, $p=.018$), excluding age. Although number of coupling events and MI explained enough variance to stay in the model, GFAP was the only term significantly explaining variance in PSI.

Plasma Aβ42/40 ratios were not explained by any of the available measures ($F(26)=1.40$, $R^2_{adj}=.01$, $p=.248$). Number of coupling phases, PSI, and age were dropped from the a-priori baseline model,

and MI remained as a non-significant predictor in the optimized model (p=.248), indicating that amyloid clearance is seemingly not related to SW-spindle coupling in healthy older adults.

In summary, these optimized models suggest a link between SW-spindle coupling and astrocyte activation: falling sleep quality- and quantity-related reduction in SW-spindle coupling events was associated with increased signs of astrocyte activation as measured by plasma GFAP levels (figs. 2&3). Increased GFAP levels in turn were paralleled by a shift in PSI resembling the physiology of younger participants. Age is not directly associated with this process, suggesting this older age subgroup to be of homogeneous age. We deliberate on potential explanations (e.g., compensatory increase in PSI in response to deteriorating neurophysiology and neural integrity) in the discussion section and fig. 4.

FIGURE 3 ABOUT HERE

FIGURE 4 ABOUT HERE

4. Discussion

We show that SW-spindle phase-amplitude coupling gradually shifts across the human lifespan without losing coupling strength. Corroborating previous reports (Mikutta et al., 2019; Muehlroth et al., 2019; Winer et al., 2019), SW drive spindles in younger individuals, representing the canonical hierarchy of top-down neocortical control of information flow (Rasch & Born, 2013; Staresina et al., 2015). However, while others report that this hierarchical structure dissipates with age (Helfrich et al., 2018), we found that the hierarchy reverses, settling into a configuration of spindles driving SW in old age. The extent of this reversal of coupling hierarchy was associated with markers for astrocyte activation.

Importantly, we demonstrate a gradual, not sudden, forward-shift of SW-spindle coupling across the adult human life, paralleling another large-sample study (McConnell et al., 2021). This gradual nature notwithstanding, this shift results in a fundamental structural change – a reversal of the order of events and thereby the hierarchical structure observed in younger adults – starting around age 40-48. In old age, spindles shift from being driven by- to driving SW. This effect was stronger, the lower the SW-subband analyzed: 0.5 Hz exhibited the strongest shift & coupling (PSI) with spindles, 1.0–1.5 Hz exhibited gradually reduced shift & coupling, and 2.0 Hz exhibited no shift/coupling, marking the transition away from SW and into the upper delta frequency band, which no longer seems to orchestrate sleep oscillations. What exactly the downstream effects of this shift regarding information flow inside the brain networks are must be speculated on, but others suggest that a precise hierarchy of SW driving spindles is not a necessity for information processing, but helps making it more efficient (Muehlroth et al., 2019). These authors find that in old age, a coupling hierarchy reminiscent of a younger brain is associated with higher structural integrity in key brain regions for memory processing (e.g. hippocampus and medial prefrontal cortex). This hints towards the existence of mechanisms for the preservation of a younger brain's physiology, or potentially for compensation of loss thereof. This dovetails with findings that lifelong learning and cognitively stimulating environments contribute to cognitive fitness and neuronal integrity, aid the clearance of amyloid beta, and may counteract cognitive decline (Brown et al., 2003; Fischer et al., 2007; Flexman, 2021; Lazarov et al., 2005).

Our subgroup analysis relating astrocyte activation, and therefore, potential neuroinflammatory processes to SW-spindle coupling provides a result that dovetails into such a model of maintenance and/or compensation. We find that age-related loss of sleep leads to reduced coupling. Reduced coupling is associated with an increase in plasma GFAP, a biomarker for astrocyte activation and a warning sign for potential impending cognitive decline and Alzheimer's disease. Interestingly, increased astrocyte activation is accompanied with a back-shift of SW-spindle coupling towards a younger brain's physiology. This back-shift, in turn, is associated with an increase in coupling strength and indirectly may lead to more coupling overall. This could be an indication that the aging brain attempts to compensate for loss of sleep and structural integrity by shifting the coupling hierarchy back into a more optimal configuration. An alternative explanation would be that the age-associated reversal of coupling hierarchy is a normal, healthy process, and a failure to do so is a sign of a suboptimal development, paralleled by astrocyte activation. However, as other studies strongly indicate that the age-related forward-shift in SW-spindle coupling physiology is a detrimental development associated with memory loss and brain atrophy (Chylinski et al., 2022; Helfrich et al., 2018; Ladenbauer et al., 2017; Muehlroth et al., 2019), we find this alternative explanation to be unlikely.

A notable contrast to previous findings (Helfrich et al., 2018) is that here, coupling strength (MI) did not change as a function of age. Our results indicate that MI does not exhibit age related changes in the mean, but rather in variance, resembling an inverted-U shaped curve, with middle age quartiles exhibiting larger variance in MI than extreme age quartiles (fig. 1B). This may lead to spurious changes in the mean: MI is right-skewed and cannot become negative. The lower variance in Q1 and Q4 thus leads to an asymmetrical absence of high (but not low) MI values that causes a lowered mean. The analysis in the original report by Helfrich et al. (2018) may have captured this effect, but its larger dynamics across the lifespan remained hidden from those authors as they only had access to distinct age groups.

The change in coupling phase with concomitant stability of coupling strength might explain why declarative memory is generally more severely impacted in aging and neurodegeneration compared to procedural memory (Tromp et al., 2015), as declarative memory has been associated with coupling phase, while procedural memory has been associated with coupling strength (Mikutta et al., 2019).

We found that the typical coupling hierarchy (as measured using PSI) of younger adults does not yet exist in our youngest age quartile, even though the overall event order typical for younger adults (spindles after SW peak, measured using rvec angle) is already established. This hints towards a dissociation between mere order of events versus the leading event exerting influence over the lagging event. This quartile spanned ages 15-26, with adolescents under the age of 18 featuring prominently. Only in the second quartile ranging ages 27-46, the canonical young adult coupling hierarchy (PSI>0) is established. Our data-driven model suggested that a non-linear relationship exists between coupling hierarchy and age, with an early “adolescent-young adult” and a later “adult lifespan” component. During the early component, the canonical hierarchy is established, peaking at age 29.2, and subsequently shifts gradually into the reported reversed hierarchy during the later component. This early component tracks with brain maturation, especially of white matter, which continues well into young adulthood of the early 20’s (Konrad et al., 2013). Paralleling our finding, a recent study found that SW-spindle coupling strength increases during childhood into adolescence and is associated with enhanced memory formation (Hahn et al., 2020). We find a similar inverted U-shaped dynamic in changing variance in coupling strength (MI) with age. Taken together, the non-linear waxing and waning of the SW-spindle coupling hierarchy and, arguably, coupling strength across the human lifespan may reflect different biological processes: maturation, plateau, and wear.

4.1. Limitations

Our study has several limitations. Although we were able to investigate a large sample of baseline sleep recordings, we were limited to a single frontal EEG derivation, and there were no behavioral tasks available to associate memory, executive functions or other cognitive domains to SW-spindle coupling. However, among other studies that did measure memory, there is a strong consensus that a “younger” SW-spindle coupling physiology is optimal for memory consolidation, and age-related changes in coupling are associated with reduced memory performance (Bastian et al., 2022; Chylinski et al., 2022; Helfrich et al., 2018; Ladenbauer et al., 2017; Mikutta et al., 2019; Muehlroth et al., 2019).

We could only assess the association of SW-spindle coupling with blood-based biomarkers in a subset of 28 older individuals. The lower statistical power of this comparatively small subset may

explain why we were not able to find an association with plasma amyloid levels. However, this lack of association between coupling and amyloid is consistent with other studies (Winer et al., 2019, 2020), even though one report finds that a forward-shift of spindles was associated with Aβ burden in the medial prefrontal cortex and memory decline (Chylinski et al., 2022). Arguably, aberrant amyloid dynamics, although predictive of cognitive decline years in advance (Beyer et al., 2022) may not be prominent enough in healthy older adults (yet) to associate with sleep-microstructural dynamics like SW-spindle coupling (Winer et al., 2020).

Based on an ample body of literature, we speculate that increased GFAP levels may be indicative of neuroinflammation (Beyer et al., 2022; Manchanda et al., 2018; Verberk et al., 2021; Xiao et al., 2022). However, GFAP levels are also associated with general and benign astrocyte activation (Verkhratsky & Nedergaard, 2018). Finally, our stepwise regression method is rather exploratory in nature. The suggested mechanistic pathway model attempting to explain the association of astrocyte activation/neuroinflammation with a “younger” coupling physiology is hypothetical, with directions of causality not resolved. We interpreted the regressor structure in a way that made sense in context of other studies. However, more research is needed to confirm or refute this model, including human intracranial recording studies for more direct physiological measurements, or animal studies directly manipulating cellular processes and assessing biomarker responses (Katsuki et al., 2022).

4.2. Conclusions and future directions

Our results generally agree with previous studies. However, the specific finding that SW-spindle coupling shifts across the human lifespan without losing coupling strength, with a reversal of the typical hierarchical coupling structure at midlife, is a novel finding in slight contrast with previous reports (Helfrich et al., 2018). It has generally been the assumption that the tight SW-spindle coupling typically seen in younger individuals becomes fuzzier in old age, but we do not see a decrease in coupling strength or a dissolution of a clear hierarchical structure of cross-frequency directionality in our data. On the contrary, we see that in the oldest age quartile, a hierarchical structure of cross-frequency directionality re-emerges, but in reversed form, with spindles driving SW. Zooming into this older age group, we find that deteriorating sleep, coupling physiology, and astrocyte activation go

hand in hand. Astrocyte activation is associated with a hierarchical back-shift of cross-frequency directionality to a younger status, potentially indicating compensation.

This assumption of compensation is exploratory and should be followed-up on with more systematic, prospective studies. However, if the model holds, it may hint towards SW-spindle coupling during sleep as a potential target for intervention against- or prevention of cognitive decline. As the process needing to be reversed (i.e., the shifting coupling hierarchy) starts to gradually, not suddenly, shift into a qualitatively different configuration at midlife, and as the GFAP/amyloid biomarker profile can be used to predict neurodegeneration up to 17 years before onset (Beyer et al., 2022), there remains ample time to intervene. This potentially enables early, low threshold, “soft” lifestyle adjustments to serve as a sufficient push in the right direction to avoid pathological trajectories, saving resources and preserving quality of life for otherwise afflicted individuals. What these adjustments might be should be investigated further, but as our model suggests a connection between total sleep time and coupling physiology, a focus on good sleep hygiene throughout one’s life would be a good starting point.

References

Bastian, L., Samanta, A., Ribeiro de Paula, D., Weber, F. D., Schoenfeld, R., Dresler, M., & Genzel, L. (2022). Spindle-slow oscillation coupling correlates with memory performance and connectivity changes in a hippocampal network after sleep. *Human Brain Mapping*, *43*(13), 3923–3943. https://doi.org/10.1002/hbm.25893

Berens, P. (2009). CircStat: A MATLAB Toolbox for Circular Statistics. *Journal of Statistical Software*, *31*, 1–21. https://doi.org/10.18637/jss.v031.i10

Beyer, L., Stocker, H., Rujescu, D., Holleczek, B., Stockmann, J., Nabers, A., Brenner, H., & Gerwert, K. (2022). Amyloid-beta misfolding and GFAP predict risk of clinical Alzheimer's disease diagnosis within 17 years. *Alzheimer's & Dementia: The Journal of the Alzheimer's Association*. https://doi.org/10.1002/alz.12745

Bigdely-Shamlo, N., Mullen, T., Kothe, C., Su, K.-M., & Robbins, K. A. (2015). The PREP pipeline: Standardized preprocessing for large-scale EEG analysis. *Frontiers in Neuroinformatics*, *9*, 16. https://doi.org/10.3389/fninf.2015.00016

Brown, J., Cooper-Kuhn, C. M., Kempermann, G., Van Praag, H., Winkler, J., Gage, F. H., & Kuhn, H. G. (2003). Enriched environment and physical activity stimulate hippocampal but not olfactory bulb neurogenesis. *European Journal of Neuroscience*, *17*(10), 2042–2046. https://doi.org/10.1046/j.1460-9568.2003.02647.x

Carrier, J., Viens, I., Poirier, G., Robillard, R., Lafortune, M., Vandewalle, G., Martin, N., Barakat, M., Paquet, J., & Filipini, D. (2011). Sleep slow wave changes during the middle years of life. *Eur J Neurosci*, *33*(4), 758–766. https://doi.org/10.1111/j.1460-9568.2010.07543.x

Chylinski, D., Van Egroo, M., Narbutas, J., Muto, V., Bahri, M. A., Berthomier, C., Salmon, E., Bastin, C., Phillips, C., Collette, F., Maquet, P., Carrier, J., Lina, J.-M., & Vandewalle, G. (2022). Timely coupling of sleep spindles and slow waves linked to early amyloid-β burden and predicts memory decline. *ELife*, *11*, e78191. https://doi.org/10.7554/eLife.78191

Delorme, A., & Makeig, S. (2004). EEGLAB: An open source toolbox for analysis of single-trial EEG dynamics including independent component analysis. *Journal of Neuroscience Methods*, *134*(1), 9–21.

Eide, P. K., Vinje, V., Pripp, A. H., Mardal, K.-A., & Ringstad, G. (2021). Sleep deprivation impairs molecular clearance from the human brain. *Brain*, *144*(3), 863–874. https://doi.org/10.1093/brain/awaa443

Fischer, A., Sananbenesi, F., Wang, X., Dobbin, M., & Tsai, L.-H. (2007). Recovery of learning and memory is associated with chromatin remodelling. *Nature*, *447*(7141), Article 7141. https://doi.org/10.1038/nature05772

Flexman, R. (2021). Lifelong Learning: *Delaware Journal of Public Health*, *7*(4), 124–127. https://doi.org/10.32481/djph.2021.09.015

Fultz, N. E., Bonmassar, G., Setsompop, K., Stickgold, R. A., Rosen, B. R., Polimeni, J. R., & Lewis, L. D. (2019). Coupled electrophysiological, hemodynamic, and cerebrospinal fluid oscillations in human sleep. *Science*, *366*(6465), 628–631. https://doi.org/10.1126/science.aax5440

Graff-Radford, N. R., Crook, J. E., Lucas, J., Boeve, B. F., Knopman, D. S., Ivnik, R. J., Smith, G. E., Younkin, L. H., Petersen, R. C., & Younkin, S. G. (2007). Association of Low Plasma Aβ42/Aβ40 Ratios With Increased Imminent Risk for Mild Cognitive Impairment and Alzheimer Disease. *Archives of Neurology*, *64*(3), 354–362. https://doi.org/10.1001/archneur.64.3.354

Hahn, M. A., Heib, D., Schabus, M., Hoedlmoser, K., & Helfrich, R. F. (2020). Slow oscillation-spindle coupling predicts enhanced memory formation from childhood to adolescence. *ELife*, *9*, e53730. https://doi.org/10.7554/eLife.53730

Helfrich, R. F., Mander, B. A., Jagust, W. J., Knight, R. T., & Walker, M. P. (2018). Old Brains Come Uncoupled in Sleep: Slow Wave-Spindle Synchrony, Brain Atrophy, and Forgetting. *Neuron*, *97*(1), 221-230.e4. https://doi.org/10.1016/j.neuron.2017.11.020

Hertenstein, E., Gabryelska, A., Spiegelhalder, K., Nissen, C., Johann, A. F., Umarova, R., Riemann, D., Baglioni, C., & Feige, B. (2018). Reference Data for Polysomnography-Measured and Subjective Sleep in Healthy Adults. *Journal of Clinical Sleep Medicine*, *14*(04), 523–532. https://doi.org/10.5664/jcsm.7036

Iber, C., Ancoli-Israel, S., Chesson, A., & Quan, S. F. (2007). *The AASM Manual for the Scoring of Sleep and Associated Events: Rules, Terminology and Technical Specifications*. American Academy of Sleep Medicine. http://www.aasmnet.org/scoringmanual/

Jiang, H., Bahramisharif, A., van Gerven, M. A. J., & Jensen, O. (2015). Measuring directionality between neuronal oscillations of different frequencies. *NeuroImage*, *118*, 359–367. https://doi.org/10.1016/j.neuroimage.2015.05.044

Ju, Y.-E. S., Ooms, S. J., Sutphen, C., Macauley, S. L., Zangrilli, M. A., Jerome, G., Fagan, A. M., Mignot, E., Zempel, J. M., Claassen, J. A. H. R., & Holtzman, D. M. (2017). Slow wave sleep disruption increases cerebrospinal fluid amyloid-β levels. *Brain*, *140*(8), 2104–2111. https://doi.org/10.1093/brain/awx148

Kang, J. E., Lim, M. M., Bateman, R. J., Lee, J. J., Smyth, L. P., Cirrito, J. R., Fujiki, N., Nishino, S., & Holtzman, D. M. (2009). Amyloid-beta dynamics are regulated by orexin and the sleep-wake cycle. *Science*, *326*(5955), 1005–1007. https://doi.org/10.1126/science.1180962

687 Katsuki, F., Gerashchenko, D., & Brown, R. E. (2022). Alterations of sleep oscillations in Alzheimer's disease: A
688 potential role for GABAergic neurons in the cortex, hippocampus, and thalamus. *Brain Research*
689 *Bulletin*, *187*, 181–198. https://doi.org/10.1016/j.brainresbull.2022.07.002
690 Konrad, K., Firk, C., & Uhlhaas, P. J. (2013). Brain Development During Adolescence. *Deutsches Ärzteblatt*
691 *International*, *110*(25), 425–431. https://doi.org/10.3238/arztebl.2013.0425
692 Ladenbauer, J., Ladenbauer, J., Külzow, N., de Boor, R., Avramova, E., Grittner, U., & Flöel, A. (2017).
693 Promoting Sleep Oscillations and Their Functional Coupling by Transcranial Stimulation Enhances
694 Memory Consolidation in Mild Cognitive Impairment. *The Journal of Neuroscience: The Official Journal*
695 *of the Society for Neuroscience*, *37*(30), 7111–7124. https://doi.org/10.1523/JNEUROSCI.0260-17.2017
696 Lazarov, O., Robinson, J., Tang, Y.-P., Hairston, I. S., Korade-Mirnics, Z., Lee, V. M.-Y., Hersh, L. B., Sapolsky,
697 R. M., Mirnics, K., & Sisodia, S. S. (2005). Environmental Enrichment Reduces Aβ Levels and Amyloid
698 Deposition in Transgenic Mice. *Cell*, *120*(5), 701–713. https://doi.org/10.1016/j.cell.2005.01.015
699 Manchanda, S., Singh, H., Kaur, T., & Kaur, G. (2018). Low-grade neuroinflammation due to chronic sleep
700 deprivation results in anxiety and learning and memory impairments. *Molecular and Cellular*
701 *Biochemistry*, *449*(1), 63–72. https://doi.org/10.1007/s11010-018-3343-7
702 Mander, B. A., Marks, S. M., Vogel, J. W., Rao, V., Lu, B., Saletin, J. M., Ancoli-Israel, S., Jagust, W. J., &
703 Walker, M. P. (2015). β-amyloid disrupts human NREM slow waves and related hippocampus-
704 dependent memory consolidation. *Nature Neuroscience*, *18*(7), 1051–1057.
705 https://doi.org/10.1038/nn.4035
706 Mander, B. A., Winer, J. R., Jagust, W. J., & Walker, M. P. (2016). Sleep: A novel mechanistic pathway,
707 biomarker, and treatment target in the pathology of Alzheimer's disease? *Trends in Neurosciences*,
708 *39*(8), 552–566. https://doi.org/10.1016/j.tins.2016.05.002
709 Mander, B. A., Winer, J. R., & Walker, M. P. (2017). Sleep and Human Aging. *Neuron*, *94*(1), 19–36.
710 https://doi.org/10.1016/j.neuron.2017.02.004
711 McConnell, B. V., Kronberg, E., Teale, P. D., Sillau, S. H., Fishback, G. M., Kaplan, R. I., Fought, A. J.,
712 Dhanasekaran, A. R., Berman, B. D., Ramos, A. R., McClure, R. L., & Bettcher, B. M. (2021). The aging
713 slow wave: A shifting amalgam of distinct slow wave and spindle coupling subtypes define slow wave
714 sleep across the human lifespan. *Sleep*, *44*(10), zsab125. https://doi.org/10.1093/sleep/zsab125
715 Mikutta, C., Feige, B., Maier, J. G., Hertenstein, E., Holz, J., Riemann, D., & Nissen, C. (2019). Phase-amplitude
716 coupling of sleep slow oscillatory and spindle activity correlates with overnight memory consolidation.
717 *Journal of Sleep Research*, *28*(6), e12835. https://doi.org/10.1111/jsr.12835

718 Mölle, M., Eschenko, O., Gais, S., Sara, S. J., & Born, J. (2009). The influence of learning on sleep slow
719 oscillations and associated spindles and ripples in humans and rats. *European Journal of Neuroscience*,
720 *29*(5), 1071–1081. https://doi.org/10.1111/j.1460-9568.2009.06654.x
721 Muehlroth, B. E., Sander, M. C., Fandakova, Y., Grandy, T. H., Rasch, B., Shing, Y. L., & Werkle-Bergner, M.
722 (2019). Precise Slow Oscillation–Spindle Coupling Promotes Memory Consolidation in Younger and
723 Older Adults. *Scientific Reports*, *9*(1), 1940. https://doi.org/10.1038/s41598-018-36557-z
724 Ohayon, M. M., Carskadon, M. A., Guilleminault, C., & Vitiello, M. V. (2004). Meta-analysis of quantitative sleep
725 parameters from childhood to old age in healthy individuals: Developing normative sleep values across
726 the human lifespan. *Sleep*, *27*(7), 1255–1273. https://doi.org/10.1093/sleep/27.7.1255
727 Oostenveld, R., Fries, P., Maris, E., & Schoffelen, J.-M. (2010). FieldTrip: Open Source Software for Advanced
728 Analysis of MEG, EEG, and Invasive Electrophysiological Data. *Computational Intelligence and*
729 *Neuroscience*, *2011*, e156869. https://doi.org/10.1155/2011/156869
730 Rasch, B., & Born, J. (2013). About Sleep's Role in Memory. *Physiological Reviews*, *93*(2), 681–766.
731 https://doi.org/10.1152/physrev.00032.2012
732 Rauchs, G., Schabus, M., Parapatics, S., Bertran, F., Clochon, P., Hot, P., Denise, P., Desgranges, B., Eustache,
733 F., Gruber, G., & Anderer, P. (2008). Is there a link between sleep changes and memory in Alzheimer's
734 disease? *Neuroreport*, *19*(11), 1159–1162. https://doi.org/10.1097/WNR.0b013e32830867c4
735 Redline, S., Kirchner, H. L., Quan, S. F., Gottlieb, D. J., Kapur, V., & Newman, A. (2004). The effects of age, sex,
736 ethnicity, and sleep-disordered breathing on sleep architecture. *Archives of Internal Medicine*, *164*(4),
737 406–418. https://doi.org/10.1001/archinte.164.4.406
738 Roh, J. H., Huang, Y., Bero, A. W., Kasten, T., Stewart, F. R., Bateman, R. J., & Holtzman, D. M. (2012).
739 Disruption of the sleep-wake cycle and diurnal fluctuation of beta-amyloid in mice with Alzheimer's
740 disease pathology. *Sci Transl Med*, *4*(150), 150ra122. https://doi.org/10.1126/scitranslmed.3004291
741 Staresina, B. P., Bergmann, T. O., Bonnefond, M., van der Meij, R., Jensen, O., Deuker, L., Elger, C. E.,
742 Axmacher, N., & Fell, J. (2015). Hierarchical nesting of slow oscillations, spindles and ripples in the
743 human hippocampus during sleep. *Nature Neuroscience*, *18*(11), 1679–1686.
744 https://doi.org/10.1038/nn.4119
745 Thijssen, E. H., Verberk, I. M. W., Vanbrabant, J., Koelewijn, A., Heijst, H., Scheltens, P., van der Flier, W.,
746 Vanderstichele, H., Stoops, E., & Teunissen, C. E. (2021). Highly specific and ultrasensitive plasma test
747 detects Abeta(1-42) and Abeta(1-40) in Alzheimer's disease. *Scientific Reports*, *11*(1), 9736.
748 https://doi.org/10.1038/s41598-021-89004-x
749 Tononi, G., & Cirelli, C. (2020). Sleep and synaptic down-selection. *European Journal of Neuroscience*, *51*(1),
750 413–421. https://doi.org/10.1111/ejn.14335

751 Tort, A. B. L., Komorowski, R., Eichenbaum, H., & Kopell, N. (2010). Measuring Phase-Amplitude Coupling
752 Between Neuronal Oscillations of Different Frequencies. *Journal of Neurophysiology*, *104*(2), 1195–
753 1210. https://doi.org/10.1152/jn.00106.2010
754 Tromp, D., Dufour, A., Lithfous, S., Pebayle, T., & Després, O. (2015). Episodic memory in normal aging and
755 Alzheimer disease: Insights from imaging and behavioral studies. *Ageing Research Reviews*, *24*, 232–
756 262. https://doi.org/10.1016/j.arr.2015.08.006
757 Varga, A. W., Wohlleber, M. E., Gimenez, S., Romero, S., Alonso, J. F., Ducca, E. L., Kam, K., Lewis, C., Tanzi,
758 E. B., Tweardy, S., Kishi, A., Parekh, A., Fischer, E., Gumb, T., Alcolea, D., Fortea, J., Lleo, A.,
759 Blennow, K., Zetterberg, H., … Osorio, R. S. (2016). Reduced Slow-Wave Sleep Is Associated with High
760 Cerebrospinal Fluid Abeta42 Levels in Cognitively Normal Elderly. *Sleep*, *39*(11), 2041–2048.
761 https://doi.org/10.5665/sleep.6240
762 Verberk, I. M. W., Laarhuis, M. B., Bosch, K. A. van den, Ebenau, J. L., Leeuwenstijn, M. van, Prins, N. D.,
763 Scheltens, P., Teunissen, C. E., & Flier, W. M. van der. (2021). Serum markers glial fibrillary acidic
764 protein and neurofilament light for prognosis and monitoring in cognitively normal older people: A
765 prospective memory clinic-based cohort study. *The Lancet Healthy Longevity*, *2*(2), e87–e95.
766 https://doi.org/10.1016/S2666-7568(20)30061-1
767 Verberk, I. M. W., Thijssen, E., Koelewijn, J., Mauroo, K., Vanbrabant, J., de Wilde, A., Zwan, M. D., Verfaillie, S.
768 C. J., Ossenkoppele, R., Barkhof, F., van Berckel, B. N. M., Scheltens, P., van der Flier, W. M., Stoops,
769 E., Vanderstichele, H. M., & Teunissen, C. E. (2020). Combination of plasma amyloid beta(1-42/1-40)
770 and glial fibrillary acidic protein strongly associates with cerebral amyloid pathology. *Alzheimer's*
771 *Research & Therapy*, *12*(1), 118. https://doi.org/10.1186/s13195-020-00682-7
772 Verkhratsky, A., & Nedergaard, M. (2018). Physiology of Astroglia. *Physiological Reviews*, *98*(1), 239–389.
773 https://doi.org/10.1152/physrev.00042.2016
774 Westerberg, C. E., Mander, B. A., Florczak, S. M., Weintraub, S., Mesulam, M. M., Zee, P. C., & Paller, K. A.
775 (2012). Concurrent impairments in sleep and memory in amnestic mild cognitive impairment. *J Int*
776 *Neuropsychol Soc*, *18*(3), 490–500. https://doi.org/10.1017/S135561771200001X
777 Winer, J. R., Mander, B. A., Helfrich, R. F., Maass, A., Harrison, T. M., Baker, S. L., Knight, R. T., Jagust, W. J.,
778 & Walker, M. P. (2019). Sleep as a Potential Biomarker of Tau and β-Amyloid Burden in the Human
779 Brain. *The Journal of Neuroscience : The Official Journal of the Society for Neuroscience*, *39*(32), 6315–
780 6324. https://doi.org/10.1523/JNEUROSCI.0503-19.2019
781 Winer, J. R., Mander, B. A., Kumar, S., Reed, M., Baker, S. L., Jagust, W. J., & Walker, M. P. (2020). Sleep
782 Disturbance Forecasts β-Amyloid Accumulation across Subsequent Years. *Current Biology*,
783 S0960982220311714. https://doi.org/10.1016/j.cub.2020.08.017

784 Wunderlin, M., Züst, M. A., Fehér, K. D., Klöppel, S., & Nissen, C. (2020). The role of slow wave sleep in the
785 development of dementia and its potential for preventative interventions. *Psychiatry Research:*
786 *Neuroimaging*, 111178. https://doi.org/10.1016/j.pscychresns.2020.111178
787 Xiao, S.-Y., Liu, Y.-J., Lu, W., Sha, Z.-W., Xu, C., Yu, Z.-H., & Lee, S.-D. (2022). Possible Neuropathology of
788 Sleep Disturbance Linking to Alzheimer's Disease: Astrocytic and Microglial Roles. *Frontiers in Cellular*
789 *Neuroscience*, *16*. https://www.frontiersin.org/articles/10.3389/fncel.2022.875138
790 Xie, L., Kang, H., Xu, Q., Chen, M. J., Liao, Y., Thiyagarajan, M., O'Donnell, J., Christensen, D. J., Nicholson, C.,
791 Iliff, J. J., Takano, T., Deane, R., & Nedergaard, M. (2013). Sleep Drives Metabolite Clearance from the
792 Adult Brain. *Science*, *342*(6156), 373–377. https://doi.org/10.1126/science.1241224
793 Zeller, C. J., Züst, M. A., Wunderlin, M., Nissen, C., & Klöppel, S. (2023). The promise of portable remote
794 auditory stimulation tools to enhance slow-wave sleep and prevent cognitive decline. *Journal of Sleep*
795 *Research*, e13818. https://doi.org/10.1111/jsr.13818
796 Zhang, Y., Ren, R., Yang, L., Zhang, H., Shi, Y., Okhravi, H. R., Vitiello, M. V., Sanford, L. D., & Tang, X. (2022).
797 Sleep in Alzheimer's disease: A systematic review and meta-analysis of polysomnographic findings.
798 *Translational Psychiatry*, *12*, 136. https://doi.org/10.1038/s41398-022-01897-y
799

800 Figure Legends

801 **Figure 1**: Slow-wave-spindle phase-amplitude coupling across the human life span. **A** Illustration of
802 measurement of slow waves (SW), spindles, and their coupling. In brief, SW and spindles are
803 detected using established duration and relative amplitude criteria (red and crimson). SW events are
804 centered on their negative peak, and each spindle event is classified as SW-coupled if it lies within
805 2.5 seconds of a SW event (green). Coupling (blue) is measured based on the SW-phase occurring at
806 the spindle peak (resultant vector angle, rvec angle; the average circular direction of spindle-SW
807 coupling events), coupling strength (modulation index, MI) and cross-frequency directionality (phase
808 slope index, PSI; the consistency of phase lag or lead between two signals). A PSI significantly
809 different from 0 suggests the leading signal drives the lagging signal. A positive PSI indicates SW
810 drive spindles, and vice versa for negative PSI. **B** MI is not associated with age across the entire
811 sample (N_{total}), indicating that coupling strength does not change with age. Consequently, the high-MI
812 subgroup analyses in panels D and F are not biased by age. The red dotted line separates high- from
813 low-MI subsets at z(ln(MI))=0. Inset bar graphs show the means of MI in age quartiles Q1-Q4. There

was no overall group difference among age quartiles (p=.27), but pairwise comparisons revealed a trend for Q2>Q4 (p=.07). **C** Circular-linear correlation of rvec angle with age across the entire sample (N_{total}=340). 0° represents the peak of the SW, ±180° the valley. While >99% of preferred coupling phases across all ages lie within the positive half-wave of the SW (i.e., between -90° to + 90°), there is a strong correlation of age and preferred coupling phase (R^2=.33). For younger individuals, spindles couple after the peak of the SW, while for older individuals, spindles couple before the peak of the SW. Inset phase histograms show the distribution of preferred coupling phases (dark bars) and all coupling events (light bars with blue outline) in age quartiles Q1-Q4. For the youngest quartile (Q1), the average preferred coupling phase (red indicator) occurs significantly after peak, while for the oldest quartile (Q4), the average preferred coupling phase occurs significantly before the peak (small red arrows and vectors). The best-fit model suggests a reversal of coupling from after- to before the SW peak at age 43.9 (green arrow). **D** Same as C, but only in individuals exhibiting strong phase preference as measured by the modulation index (MI) between spindles and SW (N_{highMI}=177; High MI = z(ln(MI))>0). In this sample, the relationship of preferred coupling phase and age is even more pronounced (R^2=.42). The best-fit model suggests a reversal at age 40.4 (green arrow), and Q3 already exhibits a significant shift of average preferred coupling phase to before the SW peak. **E** PSI between slow waves and spindles as a function of age. Nine data were excluded due to unstable estimates (N_{PSI}=331). A significant linear regression reveals a gradual reversal from SW leading spindles in younger individuals to spindles leading SW in older individuals (R^2=.03). When controlling for an age-related change in up-phase duration, this relationship becomes more pronounced ($R^2_{partial}$=.05). The best-fit model suggests a reversal at age 43.2. The inset bar graph shows age quartile means, t-tested against 0. Notably, the youngest quartile (Q1) does not show clear cross-frequency directionality, but Q2 and the oldest quartile (Q4) do in line with the findings in C & D. A stepwise linear model fitting higher-order polynomials resulted in a best fit using a cubic relationship (R^2_{adj}=.07, blue curve), suggesting a rising- and falling PSI across age (peaking at age 29.2), potentially reflecting brain maturation processes in adolescents. **F** Same as C, but only in individuals exhibiting strong phase preference as measured by the modulation index (MI) between spindles and SW. In this sample, the relationship of PSI and age is more pronounced (linear: R^2=.07; linear, controlling for up-phase duration: $R^2_{partial}$=.09; cubic: R^2_{adj}=.14). The best-fit model suggests a reversal

between age 44.5 (linear, green arrow) and 48.1 (cubic, blue arrow). Note: for cubic relationships in E and F, data above age 73 were excluded to prevent overfitting. *p<.05, **p<.01, ***p<.001.

Figure 2: Cross-frequency directionality as measured using phase slope index (PSI) between slow wave (SW) subbands (0.5, 1.0, 1.5, 2.0 Hz) and spindles (12-16 Hz) as a function of age. Nine data were excluded due to unstable PSI estimates (N=331). Coupling between SW and spindles is strongest for the lowest SW-frequency subband and gradually diminishes with increasing subband frequency, until it no longer is present for 2.0 Hz, marking the transition away from SW into delta frequency. Significant linear regressions, controlling for SW up-phase duration, show the reversal from SW leading spindles in younger individuals to spindles leading SW in older individuals for subbands 0.5, 1.0, and 1.5 Hz, but not 2.0 Hz (black lines). Cubic relationships follow the same trend (blue curves), suggesting a rising- and falling PSI between SW and spindles across age for SW frequencies 1.5 Hz and lower. The lower the SW subband, the stronger the association. There is no linear or cubic association between age and PSI for the highest subband (2.0 Hz), which marks the transition away from SW into delta frequency range. Boxplots show age quartiles (Q1-4), t-tested against 0 (FDR-corrected). *p<.05, **p<.01, ***p<.001, ns p>.1.

Figure 3: Association of number of slow wave (SW)-spindle coupling events (N coupling events, blue) and phase slope index (PSI, red) with plasma glial fibrillary acidic protein (GFAP) levels in older subgroup with biomarker measurements (N=28, age 61-80). N coupling events and PSI significantly predict GFAP levels in an optimized linear regression (model: $F(25)=6.45$, $R^2_{adj}=.29$, $p=.006$, see t-values for regressors in plot). No other terms were included during stepwise model optimization – i.e., age, gender, sleep parameters and MI do not contribute to explaining GFAP levels. *p<.05

Figure 4: Regressor structure of optimized linear models in older subgroup with biomarker measurements (N=28, age 61-80). Models were calculated for linear slow wave (SW)-spindle coupling measures (phase slope index, PSI; modulation index, MI; number of SW-spindle coupling events, N coupling events; in blue) and plasma glial fibrillary acidic protein levels (GFAP, a biomarker for astrocyte activation; in red). Additional variables are total sleep time (TST) and age, in gray. Pointer lines indicate regressors for pointees. Arrows are positive associations, T-ends are negative

associations. Black lines are significant regressors (p<.05), the solid gray line is a trend (p=.096), and gray dotted lines are non-significant regressors explaining enough variance to remain in models (i.e., model R^2 would drop by >.05 if removed). The converging pointer from GFAP and PSI to MI indicates the significant interaction GFAP*PSI on MI. We hypothesize the following model to explain this regressor structure: ① With age, sleep becomes fragmented, reducing the available time for SW-spindle coupling to occur. ② The reduction in N coupling events is associated with a decrease in MI and ③ an increase in plasma GFAP, suggesting decreased coupling quality and increased astrocyte activation, potentially due to deteriorating neural integrity. ④ Notably, an increase of plasma GFAP is associated with an increase in PSI, suggesting a astrocyte activation-associated shift of coupling phase towards the physiology of a younger brain. ⑤ This shift, in interaction with the increase in GFAP, is in turn associated with an increase in coupling strength (MI), ⑥ which is positively associated with N coupling events. The positive association between PSI and GFAP ④ is unexpected and may be explained in two ways: A) Coupling phase (PSI) is back-shifted towards a “younger” state to compensate for the suboptimal development of sleep quality, coupling physiology and astrocyte activation. This back-shift improves coupling strength directly and may indirectly lead to more overall coupling (N coupling events). B) Alternatively, the forward-shifted coupling phase observed across the human lifespan (see fig. 1) is a normal physiological process, and a lack of this shift (as indexed by an age-relative positive PSI) is suboptimal and associated with astrocyte activation. We favor the compensatory explanation (A) because the age-associated forward-shift in coupling phase has been shown to be associated with neurodegeneration (Helfrich et al., 2018), and an age-relative back-shift has been associated with improved brain integrity and memory (Muehlroth et al., 2019).

Tables

Table 1: Sleep parameters

	ALL (N = 340)	Q1 (age 15-27, N = 84)	Q2 (age 28-46, N = 85)	Q3 (age 47-56, N = 85)	Q4 (age 57-83, N = 86)	R^2_{age}
SPT hrs	7.8 ± 0.8	8.4 ± 0.5	7.7 ± 0.3	7.6 ± 0.8	7.6 ± 1.0	.14↓
TST hrs	7.0 ± 1.0	7.9 ± 0.6	7.0 ± 0.6	6.8 ± 0.8	6.2 ± 1.1	.43↓
SL hrs	0.9 ± 0.8	0.6 ± 0.7	0.9 ± 0.8	1.0 ± 0.8	0.9 ± 1.0	<.01
Wake %	11.1 ± 8.3	5.2 ± 3.9	9.7 ± 5.7	11.1 ± 6.1	18.4 ± 10.0	.37↑
Stage N1 %	9.7 ± 6.7	5.6 ± 2.9	7.8 ± 3.7	10.5 ± 6.6	14.9 ± 8.0	.31↑
Stage N2 %	50.1 ± 9.5	47.4 ± 7.5	53.8 ± 6.7	53.3 ± 7.9	45.8 ± 12.3	<.01
Stage N3 %	10.5 ± 9.5	21.3 ± 8.8	8.5 ± 7.1	6.3 ± 6.4	5.8 ± 6.2	.38↓
Stage R %	18.6 ± 5.0	20.5 ± 4.3	20.2 ± 4.0	18.8 ± 4.9	15.1 ± 4.9	.18↓
SE %	88.9 ± 8.3	94.8 ± 3.9	90.3 ± 5.7	88.9 ± 6.1	81.6 ± 10.0	.37↓
SD	9.3 ± 1.6	10.4 ± 0.8	9.8 ± 1.2	9.2 ± 1.4	7.8 ± 1.4	.41↓
SW amp	60.6 ± 25.6	84.9 ± 22.1	58.1 ± 25.6	47.8 ± 15.8	51.9 ± 20.1	.25↓
NCE ($\times 10^3$)	1.8 ± 0.6	2.3 ± 0.4	1.8 ± 0.4	1.7 ± 0.5	1.2 ± 0.5	.48↓

Note: Sleep period time (SPT), total sleep time (TST) and sleep latency (SL) in hours (hrs). Sleep stages (N1-3, R) and intermittent wakefulness (Wake) as a percentage of SPT, sleep efficiency (SE) as percentage of sleep during bedtime, spindle density (SD) during N2/N3 in spindle events per minute, slow wave amplitude (SW amp) in μV, number of coupling events (NCE) in thousands, all *M*±*SD*. The first data column represents the whole sample (N=340), the columns "Q1-Q4" represent age quartiles Q1-Q4 of the whole sample. The last column indicates age trends and explained variance by age (R^2_{age}, Pearson's determination coefficient). ↓ trending down, p<.001; ↑ trending up, p<.001.

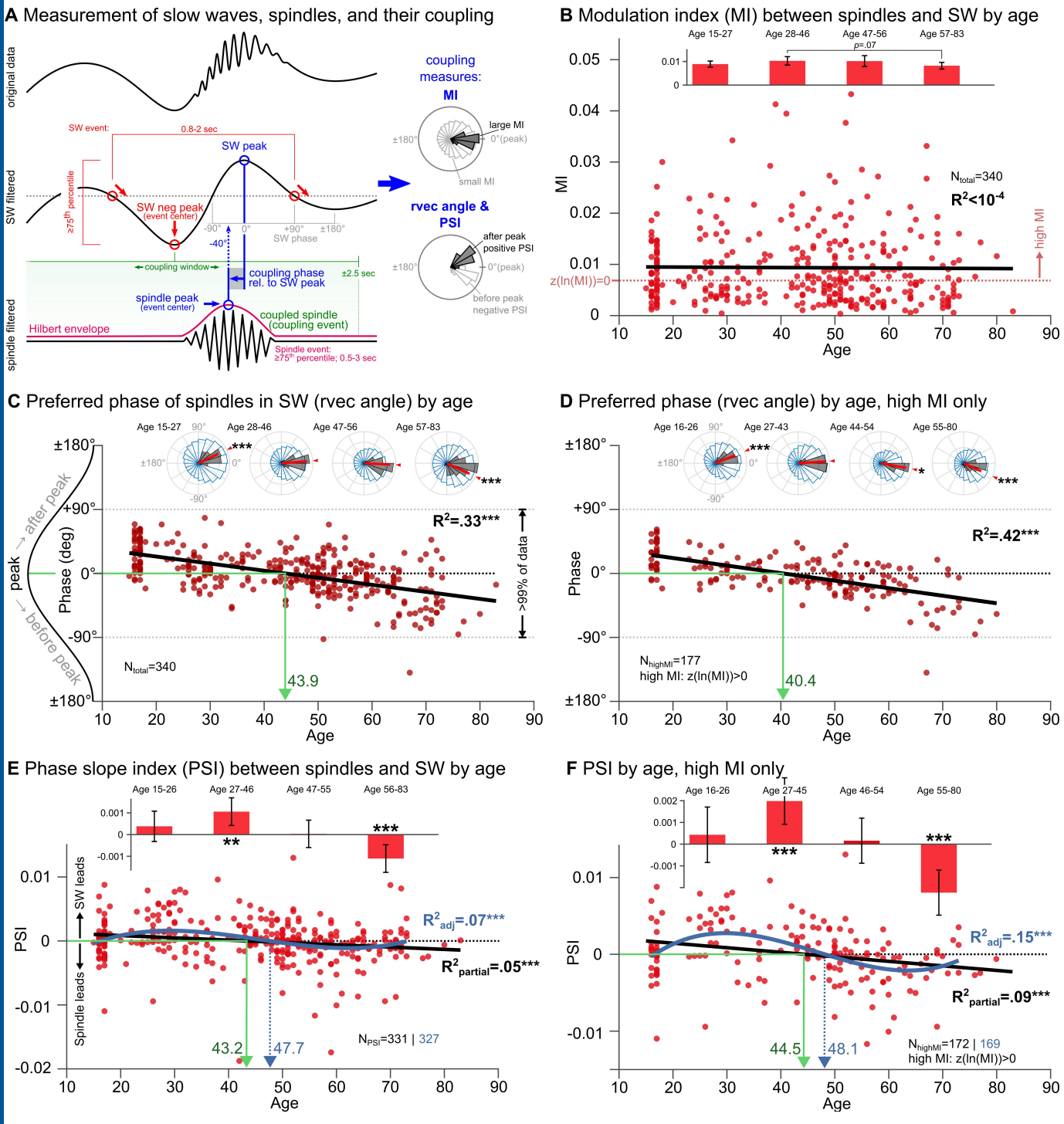

Phase slope index (PSI) between spindles and SW subbands by age